Chapter 9

# Magnetic Line Source Diffraction by a PEMC Step in Lossy Medium

Saeed Ahmed and Mona Lisa

Additional information is available at the end of the chapter

http://dx.doi.org/10.5772/intechopen.74938

**Abstract**

In this chapter, we investigate a magnetic line source diffraction problem concerned with a step. To study the diffraction problem in lossy medium, we follow the Wiener-Hopf technique and steepest decent method to solve it for impedance step. By equating the impedances of the step to zero, the solution reduces for magnetic line source diffraction by PEC step. Then we transform the obtained solution for PEMC step by using duality transformation. Perfect electromagnetic conductor (PEMC) theory is novel idea developed by Lindell and Sihvola. This media is interlinked with two conductors namely perfect electric conductor (PEC) and perfect magnetic conductor (PMC). Both PEC and PMC are the limiting cases of perfect electromagnetic conductor (PEMC). We study the magnetic line source diffraction by PEMC step placed in different soils (i) gravel sand (ii) sand and (iii) clay. By using the permittivity, permeability and conductivity of these lossy mediums we predict the loss effect on the diffracted field. Such kind of study is very useful in antenna and wave propagation for subsurface targets and to investigate antenna radiation patterns.

**Keywords:** Wiener-Hopf technique, Fourier transform, Green function, impedance, diffraction, line source, step, PEMC, PMC, PEC, Lossy medium, permeability, conductivity, permittivity

## 1. Introduction

In this chapter, we have studied the diffraction problem precisely and investigated the magnetic line source diffraction by a perfect electromagnetic conductor (PEMC) step [1–3] for the lossy medium. PEMC step is assumed to be placed in lossy medium. Discontinuity in diffraction theory is relevant to many engineering applications. The physical significance of the step

problem regarding engineering application is due to the fact that it is used in many electronic devices such as solder pad which have many applications in them which are interconnected through a step like circuit, microwave oven etc. This configuration is significant for predicting the scattering caused by an abrupt change in the material as well as in the geometrical properties of a surface. This problem is concerned with the diffraction of plane, cylindrical and surface waves by different impedance step discontinuities, such as step discontinuities made of plasmonic materials. Specially diffraction by a step in a perfectly conducting plane makes a canonical problem for the geometrical theory of diffraction (GTD) analysis of scattering by metallic tapes on paneled compact range reflectors [4]. The scattering of surface waves by the junction of two semi-infinite planes joined together by a step was first introduced by Johansen [5] in the case where both the half planes and the step are characterized by the same surface impedances. This problem is solved by using Wiener-Hopf technique, Green function and steepest descent method. The diffracted far field is investigated by the method of steepest descent. Some of the other researchers like Büyükaksoy and Birbir, Büyükaksoy and Tayyar, Büyükaksoy and Tayyar, Aksoy and Alkumru [6–16] have been investigated the scattering problems which can also be considered for the diffraction of plane, cylindrical and surface waves by different impedance step discontinuities, such as step discontinuities made of plasmonic materials.

The importance of present work stems from the facts that: (a) the scattering properties of a surface are functions of both its geometrical and material properties. (b) The edge scattering by dihedral structures whose surfaces can be modeled by the impedance boundary condition has been the focus of attention of many scientists for both acoustic and electromagnetic waves [17]. (c) The step geometry constitutes a canonical problem for scattering because a step geometry is used as an interconnection circuit of many electronic devices such as solder pad, microwave oven and frequency selective surface etc. [18]. A diffraction problem due to a magnetic line source is considered as better substitute than the plane waves. It is pertinent to mention here that the problem of diffraction of plane or line source diffraction of electromagnetic waves from a step is both mathematically difficult and physically important because the solution of the problem involves determination of $n$ unknowns which in turn requires the solution of system of $n$ linear equations.

It is clear that in the case of the line source incidence, the results of plane wave diffraction by impedance step are modified by a multiplicative factor of the form $\left(\frac{2\pi}{k\rho_0}\right)^{\frac{1}{2}}\exp\left(ik\rho_0 + i\frac{\pi}{4}\right)$, which agrees with the results already known [19, 20]. In far zone, the solution of magnetic line source diffraction reduces to plane wave as $k\rho \to \infty$. Using the method described in [16], the concerned problem "magnetic line source diffraction by an impedance step" is first reduced to a modified Wiener-Hopf equation of the second kind whose solution contains infinitely many constants satisfying an infinite system of linear algebraic equations. From this far field solution we obtain analytical solution for magnetic line source diffraction by perfect electric conductor (PEC) step, by taking the surface impedances $\eta_1$ and $\eta_2$ equal to zero. Next, we apply the duality transformation introduced by Lindell and Sihvola. Transformations have been made from the diffracted fields by a PEC step plane to PEMC step. Numerical solution of this system is obtained for various values of parameter $M$ with

step height $a = \lambda/4$, from which the effects of these parameters on the diffraction phenomenon are studied and compared with the PEMC analytical theory [3]. Next we study the solution magnetic line source diffraction by PEMC step. PEMC is novel metamaterial developed by Lindell and Sihvola [21, 22]. Its constitutive relations and salient features are given below:

$$(i)\ \mathbf{D} = M\mathbf{B}$$

and

$$(ii)\ \mathbf{H} = -M\mathbf{E}$$

PEMC behaves as an example of an ideal boundary. As a check, we obtain the PMC and PEC boundary conditions as the two limiting case of PEMC:

$$M \to 0\ (PMC) : \mathbf{n} \times \mathbf{H} = 0,\ \ \mathbf{n}.\mathbf{D} = 0$$

and

$$M \to \pm\infty(PEC) : \mathbf{n} \times \mathbf{E} = 0,\ \ \mathbf{n} \cdot B = 0.$$

This medium is characterized by a scalar parameter M known as admittance of the surface. PEMC is a generalization of both perfect electric conductor (PEC) and perfect magnetic conductor (PMC) media. Therefore, the medium is known as PEMC. Defining a certain class of duality transformations, this medium corresponds to PEC or PMC media. PEMC medium allows some nonzero fields, it rejects electromagnetic field propagation and acts as a boundary to electromagnetic waves just like the PEC and PMC media. Denoting the unit normal between air and PEMC by, from the continuity of tangential component, the electric field **E** and the magnetic field **H** satisfy the equation

$$\mathbf{H} + M\mathbf{E} = 0$$

It is also continuous through the PEMC air interface, because this vanishes in the PEMC medium, and the boundary condition becomes

$$\mathbf{n} \times (\mathbf{H} + M\mathbf{E}) = 0$$

Similarly, the normal component of the field satisfies

$$\mathbf{D} - M\mathbf{B} = 0$$

and is continuous across the boundary for

$$\mathbf{n} \cdot (\mathbf{D} - M\mathbf{B}) = 0.$$

Because the normal component of the Poynting vector at the PEMC boundary vanishes and is nonreciprocal, except in the PMC and PEC limiting cases $M = 0, \pm\infty$ respectively. PEMC

is truly isotropic, but due to the cross-components in addition to the co-components in the scattered field, it is bi-isotropic. Due to its particular property of short-circuiting a linear combination of the tangential electric and magnetic fields, the PEMC media can be exploited in microwave engineering applications. Some examples of such are, e.g., ground planes for low-profile antennas, field pattern purifiers for aperture antennas, polarization transformers, radar reflectors, and generalized high-impedance surfaces. PEMC medium can be artificially constructed by building a structure which forces the boundary conditions on the surface of a sample to be the same as those of PEMC. Many authors have worked on PEMC and metamaterial [21–47]. Next we will study the magnetic line diffraction by PEMC step in lossy medium and the fields are obtained analytically for more general solution.

We extend the problem reported by [3] for the lossy background medium. Several canonical objects in lossy media has been investigated over the years by many authors [44–56] by applying approximate values of electric conductivity and dielectric constants of various materials. The concept of subsurface scattering of EM waves for detecting the cavities and targets buried in soil has important applications in the areas of nonproliferation of weapons, environmental monitoring, hazardous-waste site location and assessment, and even archeology. To have information about this potential, it is first essential to understand the behavior of the soil by applying EM wave, and how the targets within the soil give response. We analyze the response of the soil to an EM wave by using complex dielectric permittivity of the soil in finding radar range resolution. This leads to a concept of an optimum frequency and bandwidth for imaging in a particular soil. The radar cross section of several canonical objects in lossy media is derived, and examples are given for several objects like scattering of buried PEC sphere, PEC cylinder, and PEC plate [44] and similarly scattering by PEMC plate [54], PEMC strip [55] and PEMC cylinder [56]. Furthermore, we can study the diffraction by PEC and PEMC half plane [39] and step is also made by semi-infinite half planes with a step height a, so they can also be investigated for diffraction by using the electric parameters of soils. Also characteristics of radar cross section can be further studied with different objects for PEC, PMC and PEMC cases in lossy medium. In addition to RCS of various PEC, PMC and PEMC objects [59] in lossy medium can also be investigated in future.

The objective of this chapter is to determine the diffracted field by PEMC step excited by a line source in lossy medium and to investigate surface and borehole techniques for detecting and mapping subsurface cavities, targets and to evaluate the results of surface and borehole radar probings performed at the test sites. Detection of subsurface cavities is concerned with ground-probing radar. A number of factors that control the velocity, absorption and attenuation characteristics of a radar wave and plane EM wave propagating through a dielectric as well as lossy medium like the earth. The imaging of objects buried in soil has potentially valuable applications in many diverse areas, such as nonproliferation of weapons, environmental monitoring, hazardous-waste site location and assessment, and even archeology. We study the magnetic line source diffraction by PEMC step placed in different soils (i) gravel sand (ii) sand and (iii) clay. By using the approximate value of permittivity, permeability and conductivity of these lossy mediums, we predict and analyze the loss effect on the diffracted field.

http://dx.doi.org/10.5772/intechopen.74938

## 2. Mathematical model

Consider the diffraction due to a magnetic line source located at $(x_0, y_0)$, illuminated by two half planes $S_1 = \{x < 0,\ y = a,\ z \in (-\infty, \infty)\}$ and $S_2 = \{x > 0,\ y = 0,\ z \in (-\infty, \infty)\}$ with relative surface impedance $\eta_1$ joined together by a step of height $"a"$ with relative surface impedance $\eta_2$. The geometry of the line source diffraction is shown in **Figure 1**.

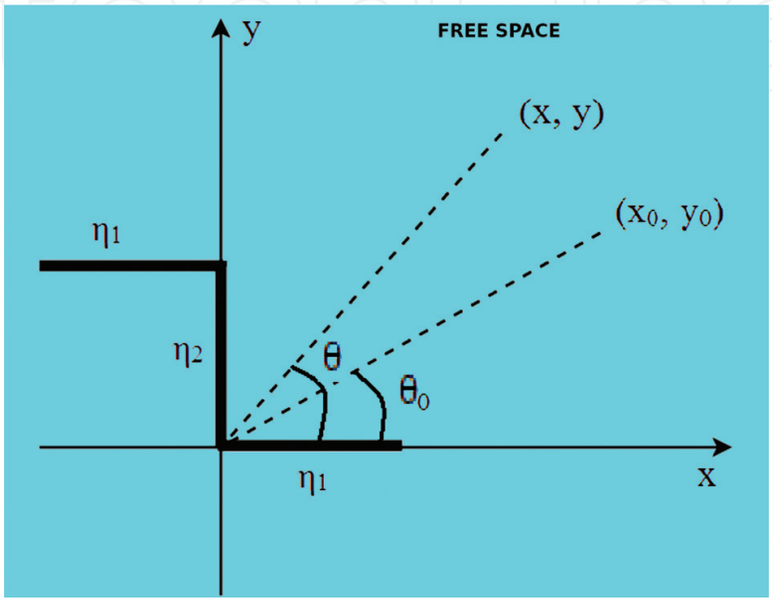


**Figure 1.** Geometry of problem: a line source located at $(x_0, y_0)$ making an angle $\theta_0$ with the horizontal, is incident upon impedance step of surface impedances $\eta_1$ and $\eta_2$, respectively, as shown. Here, $(x, y)$ is the observation point at an angle $\theta$ with the horizontal.

The time dependence $e^{-i\omega t}$, is suppressed throughout the solution.

The Helmholtz equation concerned with the diffraction problem is given below

$$\left(\frac{\partial^2}{\partial x^2} + \frac{\partial^2}{\partial y^2} + k^2\right) u^T(x, y) = \delta(x - x_0)\delta(y - y_0), \tag{1}$$

subject to the boundary conditions at two half planes and a step given by:

## 3. Boundary conditions

$$\left[1 + \frac{\eta_1}{ik}\frac{\partial}{\partial y}\right] u^T(x, a) = 0, \quad x < 0 \tag{2}$$

$$\left[1 + \frac{\eta_2}{ik}\frac{\partial}{\partial x}\right] u^T(0, y) = 0, \quad 0 < y < a \tag{3}$$

and

$$\left[1+\frac{\eta_1}{ik}\frac{\partial}{\partial y}\right]u^T(x,0)=0,\quad x>0 \tag{4}$$

with continuity equations:

$$u^T(x,a^-)=u^T(x,a^+) \tag{5}$$

and

$$\frac{\partial u^T(x,a^-)}{\partial y}=\frac{\partial u^T(x,a^+)}{\partial y} \tag{6}$$

where $u^T$ is the total field. For the mathematical analysis purpose, it is easy to express the total field $u^T(x,y)$ as follows:

$$u^T(x,y)=\begin{cases} u_i(x,y)+u_1^r(x,y)+u_1(x,y), & y>a, \\ u_2(x,y), 0<y<a, \end{cases} \tag{7}$$

Here, $k=\omega/c$ is the wave number and supposed to have positive imaginary part. The lossless case can be obtained by making $Imk\to 0$ in the final expressions. By substituting Eq. (7) in Eqs. (1)–(6), we arrive at

$$\left(\frac{\partial^2}{\partial x^2}+\frac{\partial^2}{\partial y^2}+k^2\right)u^i(x,y)=\delta(x-x_0)\delta\left(y-y_0\right). \tag{8}$$

and

$$\left(\frac{\partial^2}{\partial x^2}+\frac{\partial^2}{\partial y^2}+k^2\right)u_1^r(x,y)=\delta(x-x_0)\delta\left(y+y_0\right). \tag{9}$$

The solution of the incident field and reflected field from [11] can be written as

$$u^i(x,y)=be^{-ik\left[x\cos\phi_0+y\sin\theta_0\right]}$$

$$u_1^r(x,y)=b\frac{\eta_1\sin\phi_0-1}{\eta_1\sin\theta_0+1}e^{-ik\left[x\cos\phi_0+(y-2a)\sin\phi_0\right]}$$

where

$$b=-\frac{1}{4i}\sqrt{\frac{2}{\pi kr_0}}e^{i(kr_0-\pi/4)}$$

The diffracted field $u_1(x,y)$ and $u_2(x,y)$ satisfy the Helmholtz equations

$$\left(\frac{\partial^2}{\partial x^2}+\frac{\partial^2}{\partial y^2}+k^2\right)u_1(x,y)=0, \qquad x\in(-\infty,\infty). \tag{10}$$

$$\left(\frac{\partial^2}{\partial x^2}+\frac{\partial^2}{\partial y^2}+k^2\right)u_2(x,y)=0, \qquad x\in(0,\infty). \tag{11}$$

$$\left[1+\frac{\eta_1}{ik}\frac{\partial}{\partial y}\right]u_1(x,a)=0, \quad x<0 \tag{12}$$

$$\left[1+\frac{\eta_2}{ik}\frac{\partial}{\partial x}\right]u_2(0,y)=0, \quad 0<y<a \tag{13}$$

and

$$\left[1+\frac{\eta_1}{ik}\frac{\partial}{\partial y}\right]u_2(x,0)=0, \quad x>0 \tag{14}$$

$$u_1(x,a^+)+\frac{2b\eta_1\sin\phi_0}{\eta_1\sin\phi_0+1}e^{-ik\left[x\cos\phi_0+a\sin\phi_0\right]}=u_2(x,a^-) \tag{15}$$

and

$$\frac{\partial u_1(x,a^+)}{\partial y}-\frac{2bik\eta_1\sin\phi_0}{\eta_1\sin\phi_0+1}e^{-ik\left[x\cos\phi_0+a\sin\phi_0\right]}=\frac{\partial u_2(x,a^-)}{\partial y} \tag{16}$$

where

$$b=-\frac{1}{4i}\sqrt{\frac{2}{\pi kr_0}}e^{i(kr_0-\pi/4)}$$

## 4. Fourier transform

Taking Fourier transform of the Eq. (10) such that:

$$\Phi(\alpha,y)=\frac{1}{\sqrt{2\pi}}\int_{-\infty}^{\infty}u_1(x,y)e^{i\alpha x}dx,$$

and

$$u_1(x,y)=\frac{1}{\sqrt{2\pi}}\int_{-\infty}^{\infty}\Phi(\alpha,y)e^{-i\alpha x}d\alpha,$$

where

$$\Phi(\alpha, y) = \Phi_-(\alpha, y) + \Phi_+(\alpha, y)$$

$$\Phi_+(\alpha, y) = \frac{1}{\sqrt{2\pi}} \int_0^\infty u_1(x, y) e^{i\alpha x} dx,$$

$$\Phi_-(\alpha, y) = \frac{1}{\sqrt{2\pi}} \int_{-\infty}^0 u_1(x, y) e^{i\alpha x} dx,$$

and Eq. (10) reduce to

$$\frac{d^2\phi}{dy^2} + \gamma^2 \phi(\alpha, y) = 0, \tag{17}$$

where $\gamma(\alpha) = \sqrt{k^2 - \alpha^2}$ and $\alpha$ is a complex transform variable.

Apply half range Fourier transforms to the Eq. (11)

$$\left[\frac{\partial^2}{\partial x^2} + \frac{\partial^2}{\partial y^2} + k^2\right] \Psi_+(\alpha, y) = 0, \quad 0 < y < a. \tag{18}$$

where

$$\Psi_+(\alpha, y) = \frac{1}{\sqrt{2\pi}} \int_0^\infty u_2(x, y) e^{i\alpha x} dx$$

Fourier transforms of the Eqs. (12)–(16) can be written as

$$\left[1 + \frac{\eta_1}{ik} \frac{\partial}{\partial y}\right] \Phi_-(\alpha, a) = 0, \quad x < 0 \tag{19}$$

$$\left[1 + \frac{\eta_2}{ik} \frac{\partial}{\partial x}\right] \Psi_+(\alpha, a) = 0, \quad 0 < y < a \tag{20}$$

and

$$\left[1 + \frac{\eta_1}{ik} \frac{\partial}{\partial y}\right] \Psi_+(\alpha, 0) = 0, \quad x > 0 \tag{21}$$

$$\Phi_-(\alpha, a^+) - \frac{H_0}{\alpha - k\cos\phi_0} = \Psi_+(x, a^-) \tag{22}$$

and

$$\frac{\partial \Phi_-(\alpha, a^+)}{\partial y} + \frac{ik}{\eta_1} \frac{H_0}{\alpha - k\cos\phi_0} = \frac{\partial \Psi_+(x, a^-)}{\partial y} \tag{23}$$

where

$$H_0 = \frac{1}{8\pi^2}\frac{2\eta_1 \sin\phi_0}{\eta_1 \sin\phi_0 + 1} e^{-ika\sin\phi_0}\frac{2\pi}{\sqrt{kr_0}} e^{i(kr_0-\pi/4)}.$$

The solution of Eq. (17) satisfying the radiation condition for $y > a$ can be written as:

$$\Phi(\alpha, y) = B(\alpha) e^{i\gamma(\alpha)|y-a|}, \tag{24}$$

where $B(\alpha)$ is the unknown coefficient to be determined by substituting $y = a$ in the following expression $\Phi_+(\alpha, y) + \Phi_-(\alpha, y)$ and $\frac{\partial\Phi_+(\alpha,y)}{\partial y} + \frac{\partial\Phi_-(\alpha,y)}{\partial y}$, and with the help of boundary condition;

$$\Phi_-(\alpha, a) + \frac{\eta_1}{ik}\Phi'_-(\alpha, a) = 0, \tag{25}$$

where prime denotes differentiation with respect to $y$.

$$R_+(\alpha) = B(\alpha)\left(1 + \frac{\eta_1}{k}\gamma(\alpha)\right), \tag{26}$$

where

$$R_+(\alpha) = \Phi_+(\alpha, a) + \frac{\eta_1}{ik}\Phi'_+(\alpha, a). \tag{27}$$

From the Eqs (22), (23), (26) and (27), we obtain the following Wiener-Hopf functional equations

$$\frac{\partial\Psi_+(x,a)}{\partial y} = \frac{R_+(\alpha)i\gamma(\alpha)}{\left(1 + \frac{\eta_1}{k}\gamma(\alpha) + \frac{ik}{\eta_1}\Phi_-(\alpha, a) + \frac{ik}{\eta_1}\frac{F_0}{\alpha - k\cos\phi_0}\right.} \tag{28}$$

The corrected solution of Wiener-Hopf equation [2] in case of line source can be expressed as

$$\begin{aligned}
&\frac{R_+(\alpha)}{(\alpha + T)G_+(\alpha)} \\
&= F_0\frac{i\eta_1}{k}\frac{(k\cos\theta_0 - T)G_-(k\cos\theta_0)}{\alpha - k\cos\theta_0} \\
&+ \frac{k}{\eta_1}\frac{\left(\frac{k}{\eta_2} - T\right)G_+(T)R_+(T)e^{-\frac{ika}{\eta_1}}}{\left(\frac{k}{\eta_2} + T\right)\sin\left(\frac{ka}{\eta_1}\right)(\alpha + T)} \\
&+ \sum_{n=1}^{\infty}\frac{\left(\frac{k}{\eta_2} - \alpha_n\right)G_+(\alpha_n)R_+(\alpha_n)\left(\frac{n\pi}{a}\right)^2}{\left(\frac{k}{\eta_2} + \alpha_n\right)a\alpha_n(T - \alpha_n)(\alpha + \alpha_n)},
\end{aligned}$$

where

$$F_0 = \frac{i}{8\pi^2}\frac{2\eta_1 \sin\theta_0}{1+\eta_1 \sin\theta_0} e^{-ika\sin\theta_0}\frac{2\pi}{\sqrt{kr_0}} e^{-i\left(kr_0-\frac{\pi}{4}\right)}.$$

and $\alpha_n, G(\alpha)$ and $G_+(\alpha)$ are defined in [11]. The function $R_+(\alpha)$ depends upon the unknown series of constants $R_+(T),\ R_+(\alpha_1),\ R_+(\alpha_2),\ R_+(\alpha_3)$…. To find an approximate value for $R_+(\alpha)$, substitute $\alpha = T, \alpha_1, \alpha_{2,\ldots,}, \alpha_m$ in Eq. (29) to get $m+1$ equations in $m+1$ unknowns. The simultaneous solution of these equations yields approximate solutions for $R_+(T),\ R_+(\alpha_1),\ R_+(\alpha_2), \ldots R_+(\alpha_m)$.

## 5. Far zone solution

The unknown constant $B(\alpha)$ can be obtained by taking inverse Fourier transform of Eq. (24), the final expression for the diffracted field is written as

$$u_1(x,y) = \frac{1}{\sqrt{2\pi}}\int_L \frac{R_+(\alpha)}{\left(1+\frac{\eta_1}{k}\gamma(\alpha)\right)} e^{i\gamma(\alpha)(y-a)} e^{-i\alpha x} d\alpha, \tag{29}$$

where $L$ is a straight line parallel to the real axis, lying in the strip $Im[k\cos\theta_0] < Im[\alpha] < Im[k]$. To determine the far field behavior of the scattered field, introducing the following substitutions $x = r\cos\theta, y - a = r\sin\theta$ and $\alpha = -k\cos(\theta + it)$, where $t$ is real. The contour of integration over $\alpha$ in Eq. (30) goes into the branch of hyperbola around $-ik$ if $\frac{\pi}{2} < \theta < \pi$. We further observe that in deforming the contour into a hyperbola the pole $\alpha = \xi$ may be crossed. If we make another transformation $\xi = k\cos(\theta_0 + it_1)$ the contour over $\xi$ also goes into a hyperbola. The two hyperbolae will not cross each other if $\theta < \theta_0$. However, if the inequality is reversed there will be a contribution from pole which, in fact, cancels the incident wave in the shadow region in [11]. Simply the asymptotic evaluation of the integral in Eq. (30) using the method of steepest descent, we find the following solution for far field diffracted by an impedance step due to a line source at a large distance from the edge:

$$u_1\left(r,\phi\right) e^{-i\pi/4} k\sin\phi R + (\alpha)\frac{e^{ikr}}{\sqrt{kr}} \tag{30}$$

## 6. Magnetic line source diffraction by PEC step

The asymptotic solution for the field diffracted by perfect electric conductor (PEC) step is obtained by equating $\left(\eta_1 = \eta_2 = 0\right)$ as

$$u_1\left(r,\phi\right) = e^{-i\pi/4} k\sin\phi\Phi_+\left(-k\cos\phi, a\right)\frac{e^{ikr}}{\sqrt{kr}} \tag{31}$$

where

$$\Phi_+(\alpha,a)=G_+(\alpha)\left[i\sin\phi_0\frac{e^{i\left(kr_0-\frac{\pi}{4}\right)}}{4\pi\sqrt{kr_0}}\frac{G_-\left(k\cos\phi_0\right)}{\alpha-k\cos\phi_0}+\sum_{n=1}^{\infty}\frac{G_+(\alpha_n)\left(\frac{n\pi}{a}\right)^2}{a\alpha_n(\alpha_n+\alpha)}\Phi_+(\alpha_n,a)\right] \tag{32}$$

and

$$G_+(\alpha)=\sqrt{a}e^{[\gamma a/\pi\ln(\alpha+i\gamma)/k]}e^{[i\alpha a/\pi(1-C+\ln(2\pi)/ka+i\pi/2)]}\times\prod_{n=1}^{\infty}\left[1-\left(\frac{ka}{n\pi}\right)^2-\frac{i\alpha a}{n\pi}\right]e^{\frac{i\alpha a}{n\pi}} \tag{33}$$

such that

$$G_-(\alpha)=G_+(-\alpha)$$

Next we transform magnetic line source diffracted field from PEC to PEMC step under the duality transformations in the [21]. The field diffracted by perfectly electric conducting (PEC) step can be transformed.

## 7. Magnetic line source diffraction by PEMC step

We obtain a solution for magnetic line source diffraction by PEMC step by applying a transformation introduced by Lindell and Sihvola, that is known as duality transformation [21]:

$$\begin{pmatrix}E_d^s\\H_d^s\end{pmatrix}=\begin{pmatrix}M\eta_0 & \eta_0\\\frac{-1}{\eta_0} & M\eta_0\end{pmatrix}\begin{pmatrix}E^s\\H^s\end{pmatrix}, \tag{34}$$

$$E_d^s=M\eta_0E^s+\eta_0H^s \tag{35}$$

$$H_d^s=-\frac{1}{\eta_0}E^s+M\eta_0H^s \tag{36}$$

where $E^s$ and $H^s$ are the diffracted fields and $E_d^s$ and $H_d^s$ are the intermediate fields obtained from the PEC step by satisfy the condition,

$$\eta_oH_d^s=-u_z\times E_d^s. \tag{37}$$

Moreover, the transformation

$$\begin{pmatrix}E\\H\end{pmatrix}=\frac{1}{(M\eta_0)^2+1}\begin{pmatrix}M\eta_0 & -\eta_0\\\frac{1}{\eta_0} & M\eta_0\end{pmatrix}\begin{pmatrix}E_d^s\\H_d^s\end{pmatrix} \tag{38}$$

gives

$$E = \frac{1}{\left(M\eta_0\right)^2 + 1}\left[\left(\left(M\eta_0\right)^2 - 1\right)E^s - 2M\eta_0 E^s\right] \tag{39}$$

$$H = \frac{1}{\left(M\eta_0\right)^2 + 1}\left[\left(\left(M\eta_0\right)^2 - 1\right)H^s - 2M\eta_0 H^s\right] \tag{40}$$

where $E$ and $H$ are the fields diffracted (scattered) by the PEMC step which is written as

$$E = \frac{1}{\left(M\eta_0\right)^2 + 1}\left[\left(\left(M\eta_0\right)^2 - 1\right)E^s - 2M\eta_0 E^s\right] \tag{41}$$

and

$$E^s = e^{-i\pi/4} k \sin\phi \Phi_+\left(-k\cos\phi, a\right)\frac{e^{ikr}}{\sqrt{kr}} \tag{42}$$

where

$$\Phi_+(\alpha, a) = G_+(\alpha)\left[ik\sin\phi_0 \frac{e^{i\left(kr_0 - \frac{\pi}{4}\right)}}{4\pi\sqrt{kr_0}}\frac{G_-\left(k\cos\phi_0\right)}{\alpha - k\cos\phi_0} + \sum_{n=1}^{\infty}\frac{G_+(\alpha_n)\left(\frac{n\pi}{a}\right)^2}{a\alpha_n(\alpha_n + \alpha)}\Phi_+(\alpha_n, a)\right] \tag{43}$$

## 8. Magnetic line source diffraction by PEMC step in lossy medium

When we study magnetic line source diffraction by PEMC step in lossy medium, we just replace free-space wave number k by $\gamma$, then the solution obtained from the PEMC step for the lossy medium can be expressed such that (**Figure 2**)

$$E = \frac{1}{\left(M\eta_0\right)^2 + 1}\left[\left(\left(M\eta_0\right)^2 - 1\right)E^s - 2M\eta_0 E^s\right] \tag{44}$$

and

$$E^s = e^{-i\pi/4} \gamma \sin\phi \Phi_+\left(-\gamma\cos\phi, a\right)\frac{e^{i\gamma r}}{\sqrt{\gamma r}} \tag{45}$$

where

$$\Phi_+(\alpha, a) = G_+(\alpha)\left[i\gamma\sin\phi_0 \frac{e^{i\left(\gamma r_0 - \frac{\pi}{4}\right)}}{4\pi\sqrt{\gamma r_0}}\frac{G_-\left(\gamma\cos\phi_0\right)}{\alpha - \gamma\cos\phi_0} + \sum_{n=1}^{\infty}\frac{G_+(\alpha_n)\left(\frac{n\pi}{a}\right)^2}{a\alpha_n(\alpha_n + \alpha)}\Phi_+(\alpha_n, a)\right] \tag{46}$$

where $\gamma = \beta - \alpha$, here $\alpha$ is attenuation factor and $\beta$ is propagation constant defined as in [57].

$$\alpha = \omega\sqrt{\varepsilon_0\mu_0}\sqrt{\frac{\varepsilon_r}{2}}\left[\sqrt{1+\left(\frac{18\sigma}{\omega\varepsilon_r\varepsilon_0}\right)^2}-1\right]^{1/2}$$

$$\beta = \omega\sqrt{\varepsilon_0\mu_0}\sqrt{\frac{\varepsilon_r}{2}}\left[\sqrt{1+\left(\frac{18\sigma}{\omega\varepsilon_r\varepsilon_0}\right)^2}+1\right]^{1/2}$$

where $\varepsilon_0$ and $\mu_0$ are the permittivity and the permeability of free space. For the hosted medium, we use three type of soil models [58] namely: (i) gravel sand having its conductivity $\sigma = 0.001$ mho/m and its relative permittivity $\varepsilon_r = 10.5\varepsilon_0$; (ii) sand: $\sigma = 0.0001$ mho/m and $\varepsilon_r = 8\varepsilon_0$ and (iii) clay: $\sigma = 0.01$ mho/m and $\varepsilon_r = 7\varepsilon_0$, respectively.

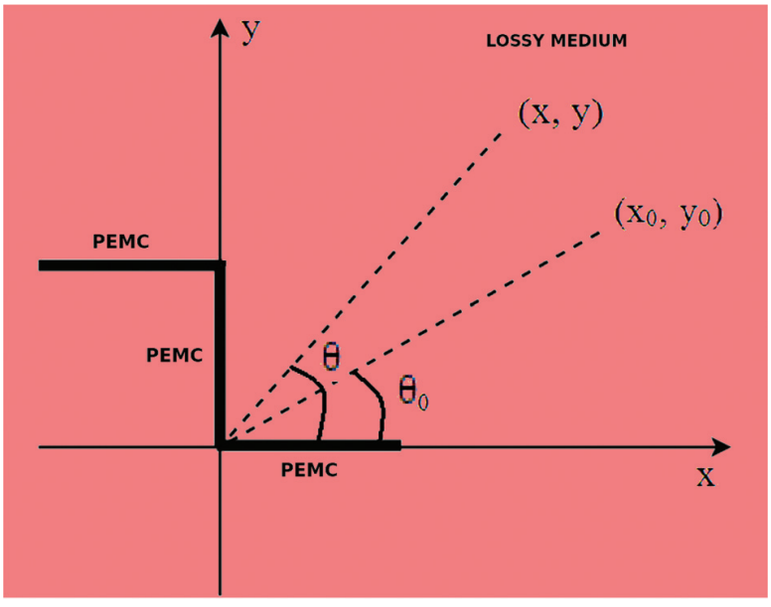


**Figure 2.** Geometry of the diffraction problem: a line source located at $(x_0, y_0)$ making an angle $\theta_0$ with the horizontal, is incident upon PEMC step surrounded by lossy medium, as illustrated in this figure. Here, $(x, y)$ is the observation point at an angle $\theta$ with the horizontal.

## 9. Results and discussion

In this section we discuss some graphical results which have been presented in [3] to predict the effects of the admittance parameters $M$ and step height $a$ and line source parameter $r_0$ on the diffraction phenomenon. It can be observed from [3] that the amplitude of the diffracted field increases with increase in step height. The graphs show that the amplitude of the diffracted field decreases as the source is taken away from the origin, which is a natural phenomenon and verifying the results. Through Mathematica software we have reproduced the results given by Lindell and Sihvola [21] and the results have retrieved. Here, an attempt is made to develop the theoretical results for lossy medium using the analytical solution for magnetic line source diffraction by PEMC step. As the step is assumed to be surrounded by different soils (i) gravel sand

(ii) sand and (iii) clay. By using the permittivity, permeability and conductivity of these lossy mediums we predict the loss effect on the diffracted field. The computed fields are obtained analytically for more general solution. The said problem is first reduced to a modified Wiener-Hopf equation of second kind whose solution contains an infinite set of constants satisfying an infinite system of linear algebraic equations. A numerical solution of this system is obtained for various values of admittance parameter $M$ and the height of the step a versus observation angle. Further, the effect of these parameters on the diffraction phenomenon is studied. It is observed that if the source is shifted to a large distance these results differ from those of by a multiplicative factor to the part of the scattered field containing the effects of incident and reflected waves. The diffraction analysis of magnetic line source by a PEMC step provides explicit formulas for electric and magnetic field amplitude and the polarization. Here, it is interesting to note that the co-polarized and the cross-polarized fields depend on the parameter $M$.

## 10. Conclusion

It is concluded that the both coupled electric and magnetic fields excitation can be observed analytically for PEMC theory that leads to a most general case for the magnetic line source diffraction by step embedded in lossy medium. The lossy medium is assumed to be made of three different soils (i) gravel sand, (ii) sand and (iii) clay. We see from their respective electric parameters namely permittivity, permeability and conductivity, as the loss increases the amplitude of the diffracted field decreases. By applying this technique to detect the subsurface targets, we can use various soil models. Further, in this chapter at a time we studied diffraction by step using PEMC theory and loss effect on the field patterns. Here, we can predict the behavior of the fields diffracted by magnetic line source. This is the most general solution and is more useful rather a plane wave solution. In far zone, we can obtain a solution for the diffraction of a plane wave by PEMC step placed in lossy medium under the condition $k\rho \to \infty$. It is also concluded that the parameter $M$ plays a significant role in PEMC theory to interlink the PEC and PMC media. The cross-polarized scattered fields vanish in the presence of PEC and PMC cases and they are maximal for $M\eta_0 = \pm 1$. If $M = \pm\infty,$ correspond to PEC case and $M = 0$, correspond to a PMC case. The impulse response of the soil is important in investigating the best operating frequency and bandwidth for a subsurface-imaging SAR. Due to dispersion and loss in the soil, the impulse response deviated from the free-space impulse response. The following conclusions can be drawn from examination of the soil's impulse response: (i) an optimum bandwidth exists; (ii) loss increases as bandwidth increases; (iii) very large bandwidths are not useful for imaging objects at large depths; (iv) vertical polarization is best for large angles of incidence and (v) lower frequencies seem best.

## Acknowledgements

The author Dr. Saeed Ahmed acknowledges the financial support from the Department of Earth Sciences, Quaid-i-Azam University, Islamabad, Pakistan, during the Post Doctoral studies for the year (20 January, 2017–19 January, 2018).

## Author details

Saeed Ahmed* and Mona Lisa

*Address all correspondence to: saeedqau@gmail.com

Department of Earth Sciences, Quaid-i-Azam University, Islamabad, Pakistan

## References

[1] Ayub M, Ramzan M, Mann AB. Magnetic line source diffraction by an impedance step. IEEE Transactions on Antennas and Propagation. 2009;**57**(4):1289-1293

[2] Ahmed S. Comments on magnetic line source diffraction by an impedance step. IEEE. 2015;**PP**(99):1

[3] Ahmed S. Magnetic line source diffraction of a plane wave by a perfectly electromagnetic conducting (PEMC) step. Journal of Modern Optics. 2014;**62**(3):175-178

[4] Sommers GA, Pathak PH. GTD solution for the diffraction by metallic tapes on paneled compact range reflectors. Proceedings of the Institution of Electrical Engineers. 1992; **139**(3):291-305

[5] Johansen E. Surface wave scattering by a step. IEEE Transactions on Antennas and Propagation. 1967;**15**(3):442-448

[6] Jamid HA, Al-Bader SJ. Reflection and transmission of surface Plasmon mode at a step discontinuity. IEEE Photonics Technology Letters. February 1997;**9**(2):220-222

[7] Valagiannopoulos CA, Uzunoglu NK. Rigorous analysis of a metallic circular post in a rectangular waveguide with step discontinuity of sidewalls. IEEE Transactions on Microwave Theory and Techniques. August 2007;**55**(8):1673-1684

[8] Yang H-Y, Alexopoulos NG. Characterization of the finline step discontinuity on anisotropic substrates. IEEE Transactions on Microwave Theory and Techniques. November 1987;**MTF35**(11):956-963

[9] Valagiannopoulos CA. High selectivity and controllability of a parallel-plate component with a filled rectangular ridge. Progress in Electromagnetics Research. 2011;**119**:497-511

[10] Pannon W, Uslenghi PLE. Exact and asymptotic scattering by a step discontinuity in an impedance plane, antennas and Propagation Society International Symposium, Houston, TX, USA. 1983; **21**. pp.13-17

[11] Büyükaksoy A, Birbir F. Plane wave diffraction by an impedance step. IEEE Transactions on Antennas and Propagation. 1993;**41**(8):1160-1164

[12] Büyükaksoy A, Birbir F. Correction to plane wave diffraction by an impedance step. IEEE Transactions on Antennas and Propagation. Mar. 1996;**44**(3):422-422

[13] Büyükaksoy A, Birbir F. Plane wave diffraction by a reactive step. International Journal of Engineering Science. 1997;**35**:311-319

[14] Büyükaksoy A, Tayyar IH. High frequency diffraction by a rectangular impedance cylinder on an impedance plane. IEE Proceedings–Science, Measurement and Technology. 2002;**149**:49-59

[15] Tayyar IH, Aksoy S, Alkumru A. Surface wave scattering by a rectangular impedance cylinder located on a reactive plane. Mathematical Methods in the Applied Sciences. 2005; **28**:525-549

[16] Noble B. Methods Based on Wiener Hopf Techniques. New York: Pergamon; 1958

[17] Rojas RG. Wiener-Hopf analysis of the EM diffraction by an impedance discontinuity in a planar surface and by an impedance half-plane. IEEE Transactions on Antennas and Propagation. 1988;**36**(1):71-83

[18] Clavel E, Schanen L, Roudet J, Arechal YM. Influence of an impedance step in interconnection inductance calculation. IEEE Transactions on Magnetics. May 1996;**32**(3)

[19] Jones DS. The Theory of Electromagnetism. London: Pergamon Press; 1964

[20] Hohmann GW. Electromagnetic scattering by conductors in the earth near a line source of current. Geophysics. 1971;**36**(1):101-131

[21] Lindell IV, Sihvola AH. Transformation method for problems involving perfect electromagnetic conductor (PEMC) structures. IEEE Transactions on Antennas and Propagation. 2005;**53**(9):3005-3011

[22] Lindell IV, Sihvola AH. Perfect electromagnetic conductor. Journal of Electromagnetic Waves and Applications. 2005;**19**:861-869

[23] Lindell IV. Electromagnetic fields in self-dual media in differential-form representation. Progress in Electromagnetics Research, PIER. 2006;**58**:319-333

[24] Ruppin R. Scattering of electromagnetic radiation by a perfect electromagnetic conductor cylinder. Journal of Electromagnetic Waves and Applications. 2006;**20**(13):1853-1860

[25] Lindell IV, Sihvola AH. Reflection and transmission of waves at the interface of perfect electromagnetic conductor (PEMC). Progress in Electromagnetics Research B. 2008;**5**: 169-183

[26] Lindell IV, Sihvola AH. Realization of the PEMC boundary. IEEE Transactions on Antennas and Propagation. 2005;**53**:3012-3018

[27] Lindell IV. Differential Forms in Electromagnetics. New York: Wiley and IEEE Press; 2004

[28] Lindell IV, Sihvola AH. Losses in PEMC boundary. IEEE Transactions on Antennas and Propagation. 2006;**54**(9):2553-2558

[29] Jancewicz B. Plane electromagnetic wave in PEMC. Journal of Electromagnetic Waves and Applications. 2006;**20**(5):647-659

[30] Lindell IV, Ruotanen LH. Duality transformations and Green dyadics for bi-anisotropic media. Journal of Electromagnetic Waves and Applications. 1998;**12**:1131-1152

[31] Lindell IV, Olyslager F. Duality in electromagnetics. Journal of Communications Technology and Electronics. 2000;**45**(2):S260-S268

[32] Ahmed S, Akbar M, Shafiq M. Diffraction by a perfectly electromagnetic conducting (PEMC) step. Journal of Modern Optics. 2013;**60**:637-640

[33] Ahmed S, Mehmood I. Diffraction of a plane wave by a perfectly electromagnetic conducting (PEMC) slot. Journal of Modern Optics. 2014;**61**:335-338

[34] Ahmed S, Manan F. Scattering by randomly placed line source in the presence of perfectly electromagnetic conducting plane. American International Journal of Contemporary Research. November 2011;**1**(3):168-172

[35] Ahmed S, Manan F. Scattering by randomly placed perfectly electromagnetic conducting half plane. International Journal of Applied Science and Technology. November 2011;**1**(6): 311-317

[36] Ahmed S, Manan F. Scattering by perfectly electromagnetic conducting random grating. American International Journal of Contemporary Research. November 2011;**1**(3):66-71

[37] Ahmed S, Manan F. Scattering by perfectly electromagnetic conducting random width strip. American International Journal of Contemporary Research. November 2011;**1**(6): 305-310

[38] Ahmed S, Manan F. Scattering by randomly placed perfectly electromagnetic conducting random width strip. International Journal of Applied Science and Technology. November 2011;**1**(6):300-304

[39] Ahmed S. Diffraction by perfect electromagnetic conductor (PEMC) half plane. International Journal of Electronics Letters. January 2017;**5**(3):255-260

[40] Ahmed S, Mann AB, Nawaz R, Tiwana MH. Diffraction of electromagnetic plane wave by a slit in a homogeneous bi-isotropic medium. Waves in Random and Complex Media. 2017;**27**(2):325-338

[41] Ahmed S. Comments on electromagnetic scattering from chiral coated nihility cylinder. Progress In Electromagnetics Research Letters. 2015;**53**:123

[42] Ahmed S. Comments on electromagnetic scattering from a chiral coated PEMC cylinder. Progress in Electromagnetics Research Letters. 2015;**53**:101

[43] Ahmed S. Comments on electromagnetic response of a circular DB cylinder in the presence of chiral and chiral nihility metamaterials. Progress in Electromagnetics Research Letters. 2015;**54**:1

[44] Brock BC, Sorensen KW. Electromagnetic Scattering from Buried Objects. Sandia National Laboratories, SAND94-2361; September 1994

[45] Kuloglu M, Chen H-C. Ground penetrating radar for tunnel detection. Geoscience and Remote Sensing Symposium (IGARSS), IEEE International, 2010;4314-4317

[46] Brock BC, Patitz WE. Optimum Frequency for Subsurface-Imaging Synthetic Aperture Radar, SAND93-0815. Springfield, USA: National Technical Information Service, US Department of Commerce; May 1993

[47] Doerry AW. A Model for Forming Airborne Synthetic Aperture Radar Images of Underground Targets, SAND94-0139. Albuquerque, New Mexico: Sandia National Laboratories; January 1994

[48] Von Hippel AR, editor. Dielectric Materials and Applications. New York: The Technology Press of M.I.T., and John Wiley & Sons, Inc.; 1954

[49] Radzevicius SJ, Daniels JJ. Ground penetrating radar polarization and scattering from cylinders. Journal of Applied Geophysics. 2000;**45**:111-125

[50] Frezza F, Pajewski L, Ponti C, Schettini G, Tedeschi N. Cylindrical-wave approach for electromagnetic scattering by subsurface metallic targets in a lossy medium. Journal of Applied Geophysics. 2013;**97**:55-59

[51] Armin WD. A Model for Forming Airborne Synthetic Aperture Radar Images of Underground Targets, Synthetic Aperture Radar Department, 2345, Sandia National Laboratories Albuquerque, NM 87185-0529, Technical Report; January 1994

[52] Bradford JH. Frequency-dependent attenuation analysis of ground-penetrating radar data. Geophysics. May–June 2007;**72**(3)

[53] Zhenhua M. Advanced Feature Based Techniques for Landmine Detection Using Ground Penetrating Radar, MS Thesis, University of Missouri-Columbia; 2007

[54] Ahmed S, Khan MK, ur Rehman A. Scattering by a perfect electromagnetic conductor plate embedded in lossy medium. International Journal of Electronics. 2015;**103**(07):1228-1235

[55] Ahmed S. The study of the radar cross section of perfect electromagnetic conductor strip. Optik. 2015;**126**(23):4191-4194

[56] Ahmed S, Rehaman AU, Zain Iftekhar M, Lisa M. Scattering by a PEMC cylinder embedded in lossy medium. Optik. 2016;**127**(19):8011-8018

[57] Ballard RB Jr. Electromagnetic (RADAR) Techniques Applied to Cavity Detection, Technical Report No. 5, Geotechnical Laboratory, P.O. BOX 631, Vicksburg, Miss. 39180; 1983

[58] Carcione JM. Ground-radar numerical modelling applied to engineering problems. European Journal of Environmental and Engineering Geophysics. 1996;**1**:65-81

[59] Rajyalakshmi P, Raju GSN. Characteristics of radar cross section with different objects. International Journal of Electronics and Communication Engineering. 2011;**4**(2):205-216